Geophysical Results at the Santo Domingo IOCG Deposit, Region III, Chile

Moul, F.[1], Witherly, K. [2]

_____
1. Condor North Consulting ULC, Vancouver, British Columbia, Canada
2. Condor Consulting Inc., Lakewood, Colorado, USA

ABSTRACT

The Santo Domingo iron oxide copper-gold (IOCG) deposit is located in the Sierra Santo Domingo, approximately 130 km northeast of Copiapó, in Region III, northern Chile. The deposit is approximately 30 km east of the Atacama Fault System which controls the occurrence of many IOCG deposits in the Chilean Iron Belt (CIB). The deposit contains total Proven and Probable Mineral Reserves of 391.7 Mt @ 0.30% Cu, 0.04 g/t Au, and 28.3% Fe (Magnetite) in three ore bodies (Santo Domingo Sur, Iris, Iris Norte) and is owned 70% by Capstone Mining Corp. (Capstone) and 30% by Korea Resources Corp.

The ore bodies are hosted in a sequence of volcanics and volcanoclastics of the Punta del Cobre Formation in contact with limestone of the Chañarcillo group. The mineralization offers a good target for gravity, magnetic, electromagnetic, and electrical methods due to shallow depth and favourable physical property contrasts relative to the country rock.

The discovery of the Santo Domingo deposit was the result of a large regional exploration effort by Far West Mining Ltd. (Far West) and BHP Billiton Ltd. The field exploration program was initiated with a regional Falcon airborne gravity-gradiometer (AGG) survey in 2002. Once interest was narrowed to the deposit area, Far West conducted several ground geophysical surveys including ground magnetics and electromagnetics (TEM). After acquiring the project, Capstone commissioned the flying of two airborne electromagnetic surveys (VTEM and ZTEM).

We present results from the airborne Falcon AGG, VTEM, and ZTEM surveys as well as the ground magnetic and TEM surveys. The methods are compared to demonstrate the efficacy in detecting the ore bodies.

INTRODUCTION

The discovery of the Santo Domingo deposit consisting of the Santo Domingo Sur (SDS), Iris (IR), Iris Norte (IN) and Estrellita (ES) iron oxide copper-gold (IOCG) orebodies was the result of a regional exploration program (the "Candelaria Project") conducted by BHP Billiton Ltd. (BHP Billiton) and Far-West Mining Ltd. (Far West). In 2002, an area of the Chilean Iron Belt (CIB) in between TalTal to approximately 75 km south of Copiapó was covered by a regional Falcon airborne gravity-gradiometer (AGG), radiometric, and magnetic geophysical survey. Between 2003 and 2005, follow-up work was conducted and the program focus was narrowed to a small group of advanced targets. In 2005, Far West drilled the discovery hole at SDS, an IOCG manto associated with gravity and magnetic anomalies. In addition to drilling off the various deposits on the property, Far West completed several ground geophysical surveys. After the project was acquired by Capstone Mining Corporation (Capstone) in 2011, two airborne electromagnetic (EM) and magnetic geophysical surveys were flown. Condor North Consulting ULC and Condor Consulting Inc. (Condor) reviewed the geophysical data for Capstone and produced an integrated interpretation (Cunion, 2014; Moul et al., 2016; Pare et al., 2016). The assembled suite of geophysical data allows characterization of the geophysical response from an IOCG deposit of the CIB.

PROJECT OWNERSHIP AND MINERAL RESERVES

The Santo Domingo (SD) project is held 70% by Capstone and 30% by Korea Resources Corporation (KORES) through the Minera Santo Domingo SCM (Minera Santo Domingo) operating entity. The project is undeveloped with total Proven and Probable Mineral Reserves of 391.7 Mt at 0.30% Cu, 0.04 g/t Au, and 28.3% Fe (Maycock et al., 2014).

LOCATION

The SD project is located in northern Chile's Coastal Cordierra approximately 130 km north-northeast of the city of Copiapó in Region III, northern Chile (Figure 1). The town of Diego de Almagro, located in the valley immediately north of the project, is connected by highway to Copiapó and to Chañaral on the Pacific coast approximately 60 km to the west. The Mantoverde and Candelaria IOCG mines are located approximately 30 km to the west-southwest and 120 km to the south-southwest, respectively.
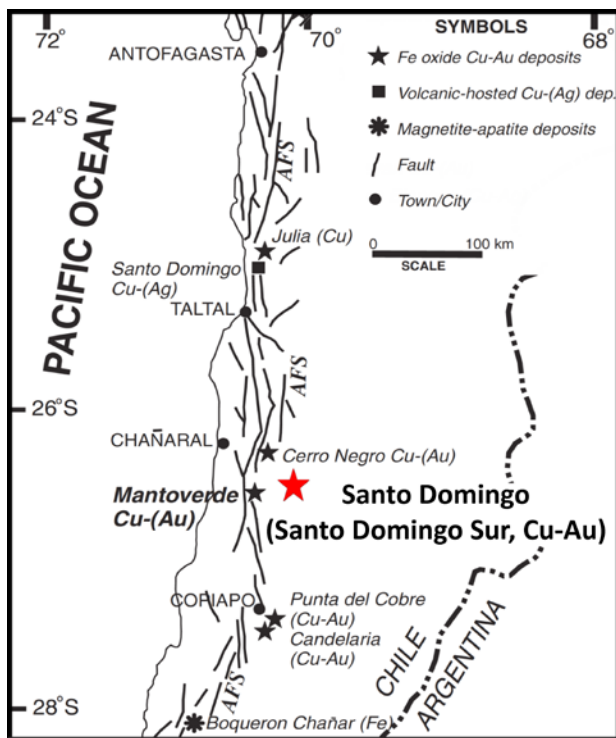
Figure 1: Location of the Santo Domingo Property relative to other IOCG deposits in regions II and III, and relative to the trace of the regional strike-slip AFS (after Benavides et al., 2007).

REGIONAL GEOLOGY

The CIB is a chain of Early Cretaceous massive iron-oxide apatite and IOCG deposits which stretch from approximately La Serena to Taltal. IOCG deposits fall into a broad group of mineralization styles which commonly contain hydrothermal iron oxides (magnetite and/or specular hematite) in addition to copper bearing iron sulphides (chalcopyrite with or without bornite) (Sillitoe, 2003). The most significant IOCG deposits (such as Candelaria-Punta del Cobre and Mantoverde) typically exhibit a combination of several mineralization styles which may include: veins, breccias, stockworks, and mantos (Sillitoe, 2003).

The geology of the area surrounding Mantoverde and the SD project (Figure 2) is dominated by volcanic and sedimentary rocks intruded by plutonic complexes (Lara and Godoy, 1998). These rocks were emplaced in an intra-arc basin related to an oblique convergent plate margin which developed during the Jurassic and Early Cretaceous (Parada et al., 2007). The volcanic and volcaniclastic rocks generated during this interval are preserved in the Punta del Cobre (Kpc) and underlying La Negra (Jln) Formations. The Lower Cretaceous Kpc is composed of a thick package of andesitic flows, intercalated tuffs, and thin sedimentary units (Lara and Godoy, 1998; cited in Benavides et al., 2007) while the middle-upper Jln is composed primarily of basaltic andesitic to andesitic flows and of lesser volcaniclastic and marine sedimentary units (Lara and Godoy, 1998; Vivallo and Henríquez, 1998; cited in Benavides et al., 2007). At

Mantoverde, the Kpc exhibits a gradational contact with the sedimentary Chañarcillo Group (Kch) (Lara and Godoy, 1998; cited in Benevides et al., 2007) indicating contemporaneous deposition.

The IOCG deposits of the CIB are closely associated with plutonic complexes. At Candelaria-Punta del Cobre and Mantoverde the deposits are closely associated with diorite and diorite and dacite dykes, respectively (Sillitoe, 2003). The intrusive events were broadly contemporaneous with the generation of fault systems including the major arc-parallel (north-south) Atacama Fault System (AFS) (Grocott and Taylor, 2002). At Mantoverde, the IOCG mineralization is directly related to the faulting as it is hosted in the Manto Verde Fault, a branch of the AFS (Vila et al., 1996; Zamora and Castillo, 2001 cited in Maksaev et al., 2007).

EXPLORATION HISTORY

The Chilean IOCG deposits became a more significant mineral resource with the discovery of the major Candelaria and Mantoverde deposits in 1986 and 1988, respectively (Maksaev et al., 2007). According to Marschik (2000) Candelaria had a resource of 470 Mt at 0.95% Cu, 0.22 g/t Au, and 3.1 g/t Ag and according to Zamora and Castillo (2001) Mantoverde had a resource of ~230 Mt at 0.55% Cu in oxides and > 400 Mt at 0.52% Cu in sulphides (both cited in Sillitoe, 2003).

According to Ryan et al. (1995), the Candelaria deposit was discovered through exploration proximal to the then producing Lar and Bronce mines. The discovery holes at Candelaria were targeted at anomalous induced polarization (IP) responses below known disseminated mineralization (though subsequent surveying showed that the polarizable areas extended into uneconomic areas associated with disseminated pyrite).

Subsequently, it was recognized that a high gradient was present in the magnetic total field across the Candelaria deposit (Ryan et al., 1995). Regional airborne magnetic surveys were completed and the Candelaria pits were shown to be coincident with highs in the reduced-to-pole (RTP) total field magnetics (Matthews and Jenkins, 1997). In general, a good correlation is observed between magnetic intensity highs and IOCG mineralization on a deposit scale, but the response may be complicated by demagnetization in massive magnetite deposits such as Candelaria (Austin et al, 2012 and 2013) and due to the highly variable susceptibility of the iron oxides present (approximately $10+$ SI and 125×10^{-5} for magnetite and specular hematite, respectively; Vella and Emerson, 2012). In the case of hematite-rich IOCG deposits such as Prominent Hill, the magnetic response may not be related to the mineralization (Hart and Freeman, 2003; cited in Austin et al., 2013).

In 2000-2002, BHP Billiton developed a concept to explore the CIB for potentially overlooked hematite-dominated IOCG mineralization using the (then proprietary) Falcon AGG and total field magnetic system (F. Bunting, pers. comm., 2017). In 2002, Far-West and BHP Billiton formed an agreement to conduct a regional exploration program (the Candelaria Project) and work was initiated later that year with a large, regional Falcon survey.
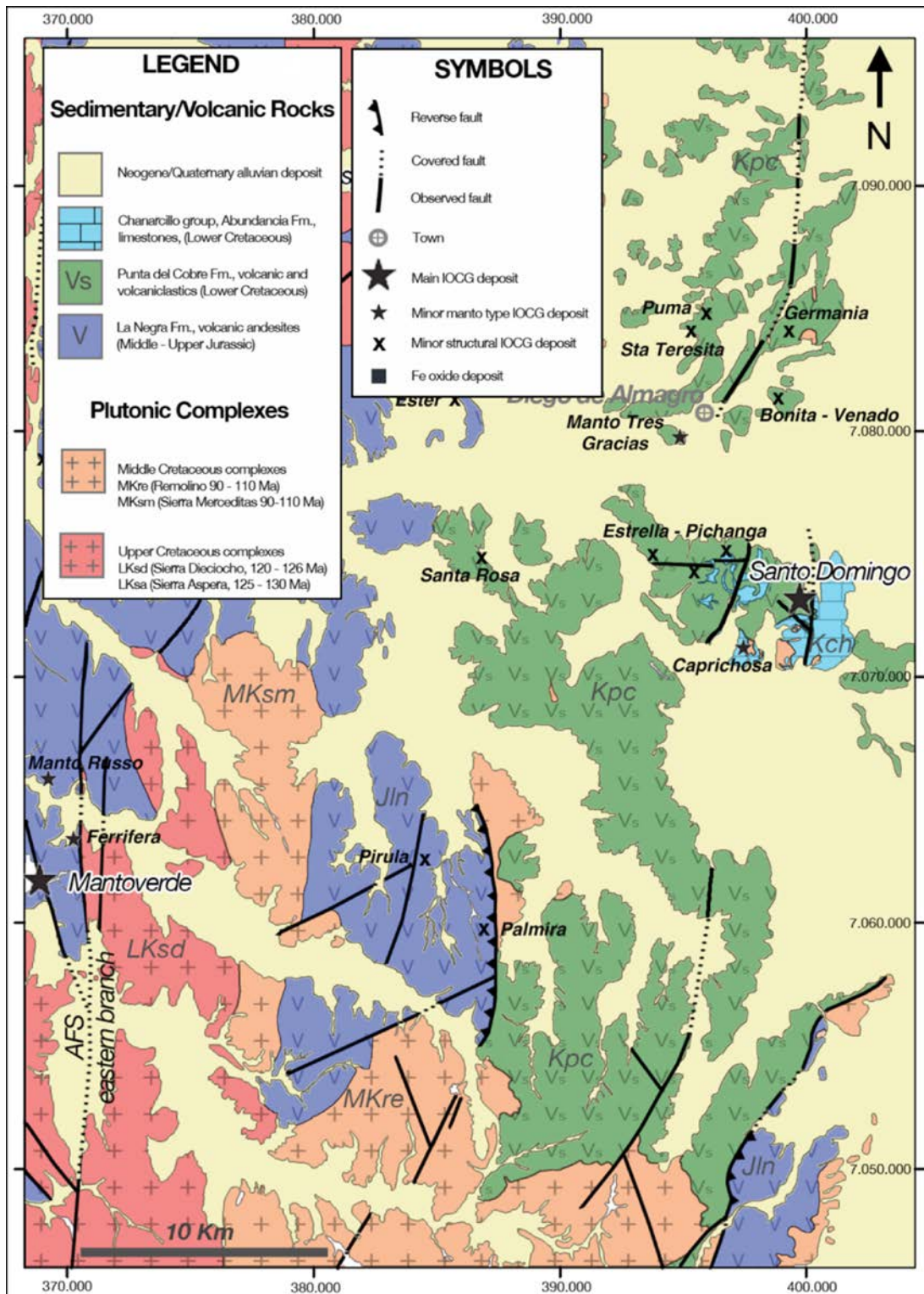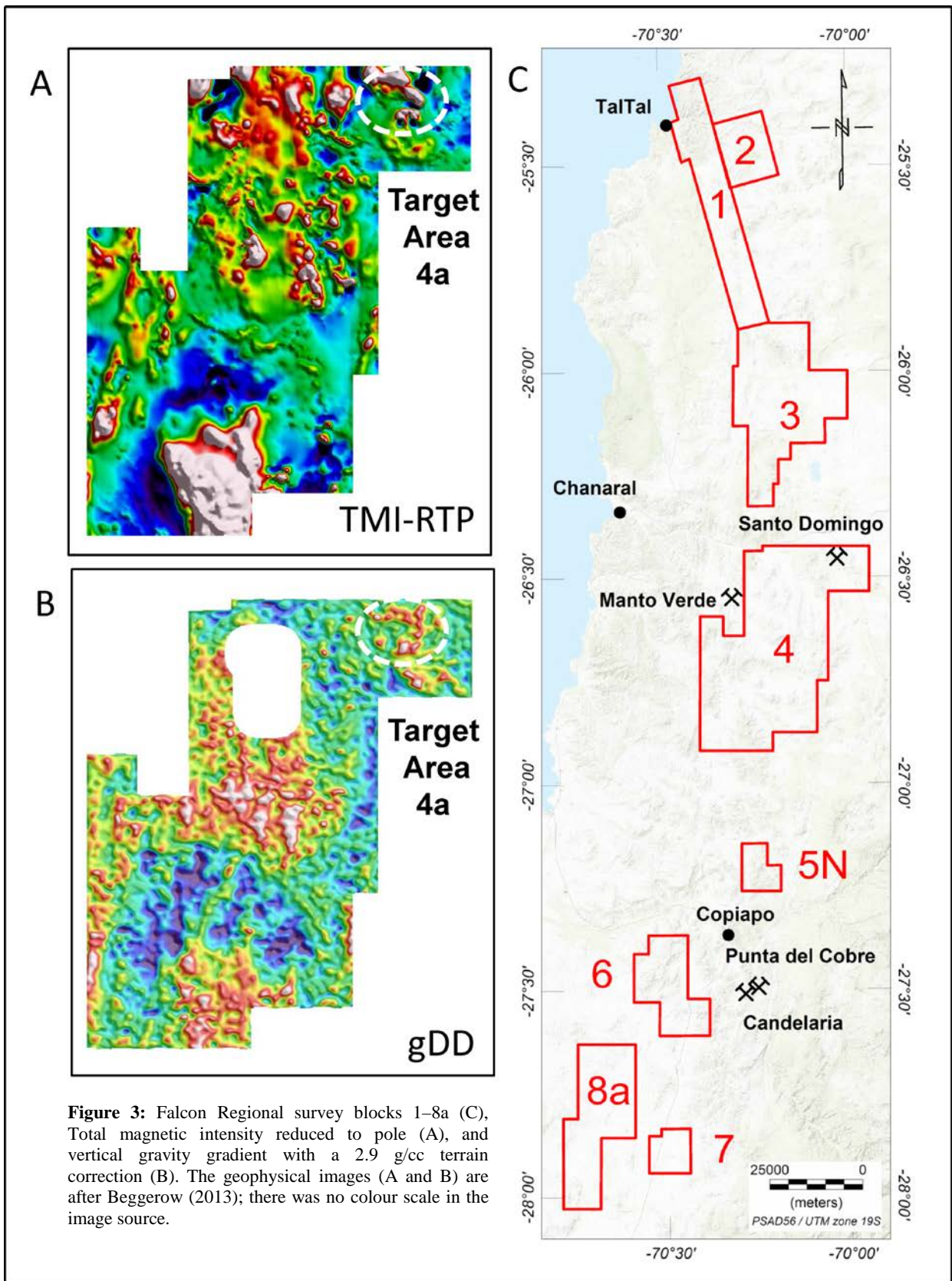
Figure 2: Regional Geology of the Mantoverde and Santo Domingo area after Daroch (2011) and Lara and Godoy (1998).

Figure 3: Falcon Regional survey blocks 1–8a (C), Total magnetic intensity reduced to pole (A), and vertical gravity gradient with a 2.9 g/cc terrain correction (B). The geophysical images (A and B) are after Beggerow (2013); there was no colour scale in the image source.

Regional Exploration Campaign

The Falcon survey consisted of a total 14,539 line-km of AGG, radiometric, and magnetic total field data acquired over eight survey blocks (McCleary, 2003) covering an approximately 300 km long section of the CIB from TalTal to approximately 75 km south of Copiapó (Figure 3). In the first interpretation of the geophysical data completed by BHP Billiton (Hensley, 2002) the exploration targets were defined primarily by vertical gravity gradient (gDD) highs but also incorporated the magnetic and radiometric results, the geology, and records of known mineralization.

BHP Billiton designated the north-east of survey block 4 was as Target Area 4a. Target 4a1, a smaller zone inside 4a, was selected based on a gDD gravity high response and an associated high K/Th ratio; neighbouring targets 4a2 and 4a3, to the southeast and the east, respectively, of 4a1, were added during subsequent review.

Follow-up and Discovery

According to Beggerow (2013), Target Area 4a was among more than 50 targets selected which were deemed to have the potential to host IOCG mineralization. Each target area was prioritized for follow-up according to metallogenic and geological data and then mapped in priority order. According to Allen (2005), early field work at 4a3 identified a broad zone of specular hematite and copper oxide-bearing veins and the active mining of a nearby copper bearing manto (Estrella, located north of ES in Figure 4). Due to the promising correlation of a gravity anomaly and mineralization at 4a3, a significant amount work was completed in the area during 2004 including an IP survey. The majority of the reverse circulation (RC) drill holes completed during the first and second drill campaigns that year were directed at chargeable zones identified from the IP survey (Allen, 2005). Most of the 21 holes intersected manto-style copper mineralization (Far West, 2005) with a promising result coming from hole 3 which intercepted 0.33% Cu over 200 m (Allen, 2005).

In May 2005, BHP Billiton elected to terminate involvement in the Candelaria Project after which Far West assumed 100% ownership with a 2% NSR retained by BHP Billiton (Hindson, 2005a). The 2005 drill campaign at 4a3 was completed later the same month and the SDS deposit was discovered with the first hole (22), which intercepted stacked manto mineralization with an interval of 0.81% copper over 56 m and 0.72% copper over a second 22 m interval at depth (Hindson, 2005b). Hole 22 was collared in the south of Target 4a3, proximal to a gDD high, and a north-northwest fault. Over the following five years, Far West consolidated ownership of properties proximal to the discoveries, drilled off the ore bodies and produced several resource estimates for the deposit. In 2011, the entire project was taken over by Capstone and KORES through the acquisition of Far-West.

PROPERTY PHYSIOGRAPHY AND GEOLOGY

The topographic variation in the SD project area is moderate, with an elevation difference of approximately 500 m between upland areas and the surrounding broad, flat valleys. The valleys are filled with thick alluvial deposits and incised fluvial channels (Figure 5). Although vegetation is sparse, bedrock is weathered and often sub-cropping with good exposures limited by the extensive overburden.

According the Daroch (2011), the ore bodies at SD are hosted by a sequence of volcanic and volcaniclastic rocks (Kpcvs, Kpcv) which are correlated with the Kpc, the Bandurrias Group (a sequence of volcanic rocks intercalated with shallow marine sediments), and a limestone-bearing volcanic section which may be the Kch (Figure 4). The volcanic units and limestone-volcanic sections are interfingered, dip approximately 15° towards the north-northwest, and are intruded by a suite of barren andesitic porphyry dykes (Kdfh). The country rocks are intruded by variably altered sills and small stocks shown as pyroxene diorite plugs and dykes (Kdi), which were a likely driver of mineralising fluids on the property.

Mineralization

The hydrothermal system found at SD resembles other IOCG deposits in the CIB (Daroch and Barton, 2011). While mineralization at SD in the Kpc occurs at a similar stratigraphic level in the Candelaria and Punta del Cobre district though Mantoverde is hosted by older volcanics of the Jln.

The main IOCG ore bodies at SD are Santo Domingo Sur (SDS), Iris (IR), and Iris Norte (IN). Daroch (2011) indicates that these three ore bodies are "physically continuous" along a roughly north-south structural trend and all three share similar host and ore mineralogy. Based on the drilled extents of the ore bodies (the outlines in the Figures 5 and 6), SDS and IR are contiguous and there is an approximately 1 km separation between IR and IN. For the purpose of this review, SDS and IR will be referred to as SDS-IR. The Estrellita (ES) orebody is located approximately 3 km northwest of SDS along an east-west structural trend referred to as the Santo Domingo Fault (SDF) which is host to at least three IOCG veins, breccias, and minor mantos (Daroch, 2011) in addition to ES.

According to Daroch (2011), the mineralization at SDS-IR and IN occurs primarily as semi- to massive specularite and magnetite mantos (greater than 50% iron minerals) which are up to 20 m thick with clots and stringers of chalcopyrite. A distinct zonation exists in SDS-IR, where an outer rim of specular-hematite grades into a magnetite-rich core (designated by "IM" in the plan view map at the top of Figure 4 with the zonation shown in the bottom section). The copper minerals are associated with the specular-hematite rim while pyrite is the dominant sulphide in the magnetite core. Mineralization in the ES orebody is in specular hematite-rich bodies and stockworks with copper oxides near surface and with minor copper-iron-sulphides located at depth.
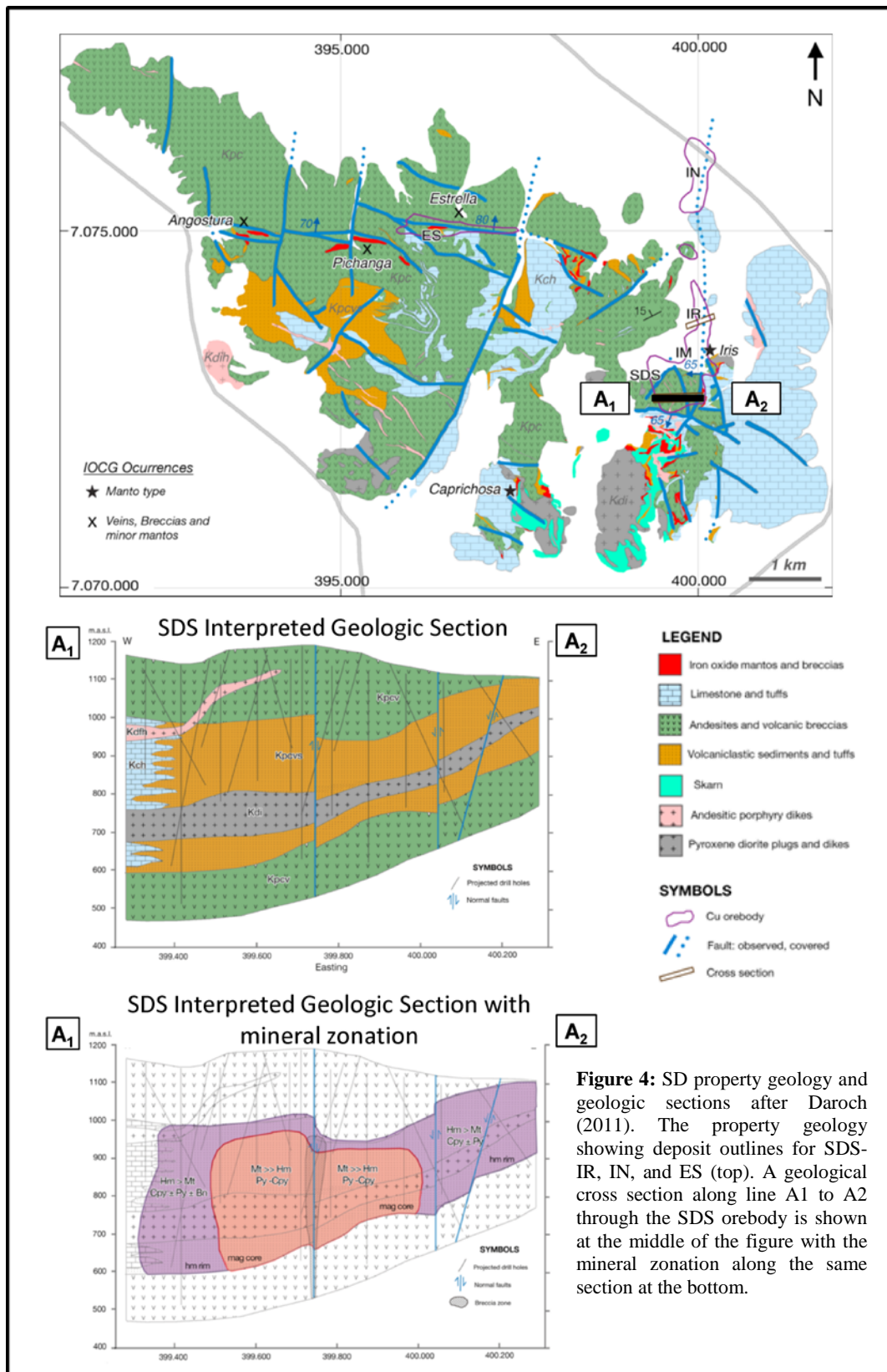
Figure 4: SD property geology and geologic sections after Daroch (2011). The property geology showing deposit outlines for SDS-IR, IN, and ES (top). A geological cross section along line A1 to A2 through the SDS orebody is shown at the middle of the figure with the mineral zonation along the same section at the bottom.
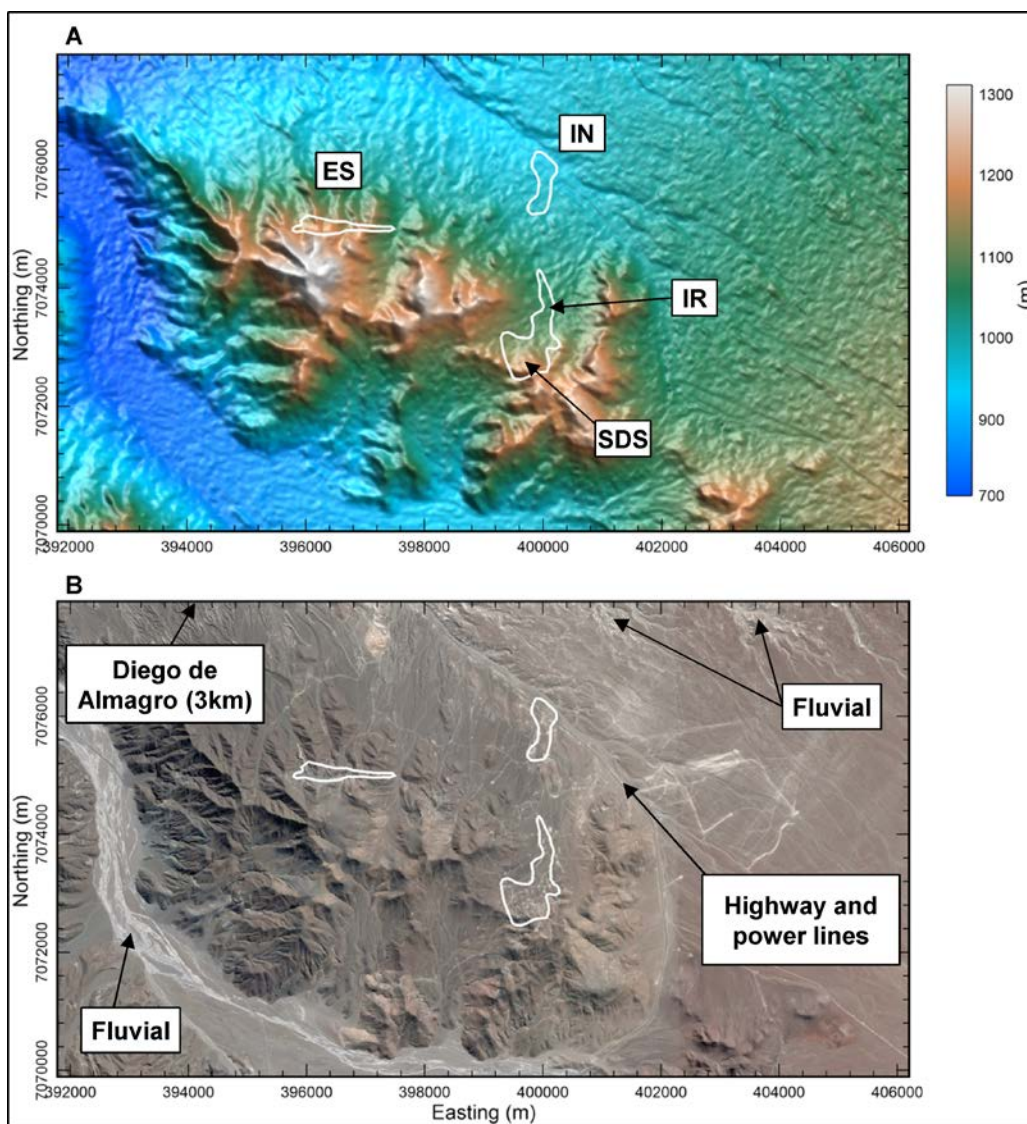
Figure 5: A panchromatic satellite image (A) and the ASTER GDEM2 digital elevation model (B) of the Santo Domingo project area (similar to the area of 4a in the previous figure). The outline of the various deposits on the property are labelled.

The numerous faults on the property exhibit significant control on the distribution of mineralization. Daroch (2011) suggests the fault displacement may be the result of reactivation along earlier structures which may have provided a path for mineralizing fluids at SDS. The east side of SDS-IR and IN is coincident with an extensive, north-south trending normal fault dipping approximately 60–70° to the west. At the south of SDS, the ore body is truncated by a northwest trending fault with dip 60° to 70° to the southwest which is the contact between the mineralized volcanics on the north and limestone to the south. At ES, the SDF dips 70° to 80° to the north and controls the mineralised occurrences surrounding the ES deposit.

In this review, we will focus on the SDS-IR, and IN ore bodies which have received the bulk of exploration work and which contribute to the most recent Mineral Reserve estimate (Maycock et al., 2014).

Physical Property Data

The presence of sedimentary rocks, intermediate volcanics of variable porosity, and intermediate intrusives which have been variably weathered and hydrothermally altered are expected to produce a wide variability in the host rock physical properties.

While no electrical conductivity or chargeability data are available, informal experiments indicate electrical continuity between sulphides along a length of massive iron-oxide dominated core (L. Beggerow, pers. comm., 2013). Although density data were acquired as part of metallurgical or engineering studies these were not available for this review.

Due to the zonation and economic value of the iron-oxides in the deposit and due to the relatively low concentration of copper in the magnetite dominant zone, magnetic susceptibility data were

systematically acquired on drill core. A suite of core samples consisting primarily of magnetite and specular hematite replacement in andesitic tuff from the SDS deposit were tested for magnetic remanence (Zonge, 2011); the median declination and inclination indicate a remnant field orientation nearly opposed to the current inducing field which is oriented north and shallowly upward (approximately -26° inclination and -2.3° declination). The mean Koenigsberger ratio was approximately 10 with a mean magnetic susceptibility 164×10^{-3} SI. Parametric modelling of the magnetic response at the south of SDS required a remnant component to return an acceptable fit to the observed response (Cunion, 2014).

We may conclude that the mantos at SDS are highly susceptible and strongly remanantly magnetized with a possible conductive zone associated with the sulphide mineralization. The IR, and IN ore bodies may have similar physical property characteristics based on the physical connection between the deposits.

GEOPHYSICS AT SANTO DOMINGO

A significant number of ground and airborne geophysical campaigns have been conducted over the SD property. Following the 2002 Falcon survey, the documented ground geophysical surveys are: a 2004 DCIP survey, a ground moving-in-loop time-domain electromagnetic survey (TEM) in 2007, and then a ground total field magnetic (TMI) survey in 2010. In 2013 and early 2014, Geotech Ltd. carried out both Versatile Time-domain Electromagnetic (VTEM) and Z-tipper Electromagnetic (ZTEM) audio-frequency magnetic (AFMAG) surveys over the property. This review concentrates on the airborne surveys as they provide more extensive, consistent, and easily accessed data coverage than the relatively sparse coverage available from the ground surveys. Selected ground survey data are used but comparison in the deposit areas were limited due to variable data quality and the common use of local position coordinates. The airborne surveys are presented in chronological order with comparison to the ground survey results where possible. In all cases, the data shown are limited to the area of current Capstone mineral dispositions.

2002 Falcon Survey

The fixed-wing Falcon acquisition and the processing of the magnetic, radiometric, and position data was completed by Sander Geophysics Ltd. (McCleary, 2003). The terrain and gravity data processing and the target selection work were completed by BHP Billiton (Hensley, 2002).

The survey consisted of eight blocks with variable line spacing and orientation (Figure 3). The majority of the SD project is covered by the Falcon survey. Block 4 consists of traverse lines at 0° with a nominal separation of 330 m and a mean, calculated, sensor (aircraft) clearance of 298 m in the SD project area. The aircraft clearance was significantly higher than the nominal 120 m claimed for the overall program due to the local terrain variation and the gentle drape required by the fixed-wing Falcon configuration.

The broad gravity high (4a) in the northwest of Block 4 contains Target Areas 4a1, 4a2, and 4a3, all of which are isolated by a 25 Eö contour of the gridded gDD with a 2.9 g/cc terrain correction

applied (Figure 6). The individual gDD highs have a good, positive correlation with the location of the known minor IOCG occurrences as well as diorite plugs, skarns, and iron-oxide mantos. All lithologies expected to have a higher density than the host volcanics and sediments. The gravity data alone are not sufficient to differentiate the ore deposits from barren rock.

The normal fault bounding the east side of SDS-IR and IN appears to be well resolved in the gravity. The fault bounding SDS on the southwest also appear to be resolved but not as clearly. The trend of the SDF is not well resolved if at all.

There is a strong, dipolar, magnetic intensity anomaly in the reduced to pole total magnetic intensity (TMI-RTP; Figure 6c) coincident with the SDS-IR deposit (approximately 1,900 nT from southern trough to peak). The related local high in the total gradient of the TMI-RTP is shifted to the south edge of SDS and is roughly coincident with the location of the discovery hole. There is a positive correlation between highs in the TMI-RTP and mapped locations of iron-oxide mantos or skarns; an exception is the high to the north of the SDF which is mapped as Kpc volcanics only. The SDF itself is well defined as an east-west local low linear feature. The contact between the Kpc and Kch at the east of SDS-IR and IN is resolved (the shift east relative to the mapped fault trace appears to be an artefact of the north-south line orientation and regional scale line spacing).

2013-2014 VTEM Survey

The heliborne VTEM survey was completed in two phases; an initial block was flown in late-2013 over the immediate area of the deposit and then in early 2014, the survey area was expanded over the surrounding dispositions. The system flown was the VTEM Max configuration at a 25 Hz base frequency with a 26 m diameter transmitter loop containing four wire turns and a peak current of 194 A. The receiver contained both Z- and X-coils and EM decays were delivered for each component between 83 µs and 10.667 ms. The survey blocks were contiguous and consisted of traverse lines nominally separated by 200 m at 130° with a mean EM sensor clearance of 46 m in the area shown. Although both magnetic and EM data were acquired, the magnetic data were not used due to sensor noise. There was increased EM noise along an approximately 500 m wide band surrounding the power transmission line in the northeast. The acquisition and processing of the EM and magnetic data were completed by Aeroquest Airborne Ltd. (wholly owned by Geotech Ltd.) (Fiset et al., 2014a, 2014b) with additional processing, inversions, and conductive plate modelling completed by Condor (Cunion, 2014). Condor generated 1D conductivity inversions and an adaptive decay time-constant (AdTau) calculation from the VTEM dB/dt Z-coil EM data.

The SDS-IR ore bodies and the south of IN are resolved as discrete high-amplitude responses in the late-time (3.521 ms) EM amplitude (dB/dt Z-coil) and as strong, isolated, relatively high time-constant features (3.5 ms) in the AdTau (Figure 7). There is no significant response associated with the ES orebody. Conductive thin-plate models through the IN and SD/IR deposits indicate typical conductance between 30 S and 90 S dipping to the northwest at approximately 20° to 30° (Cunion, 2014).
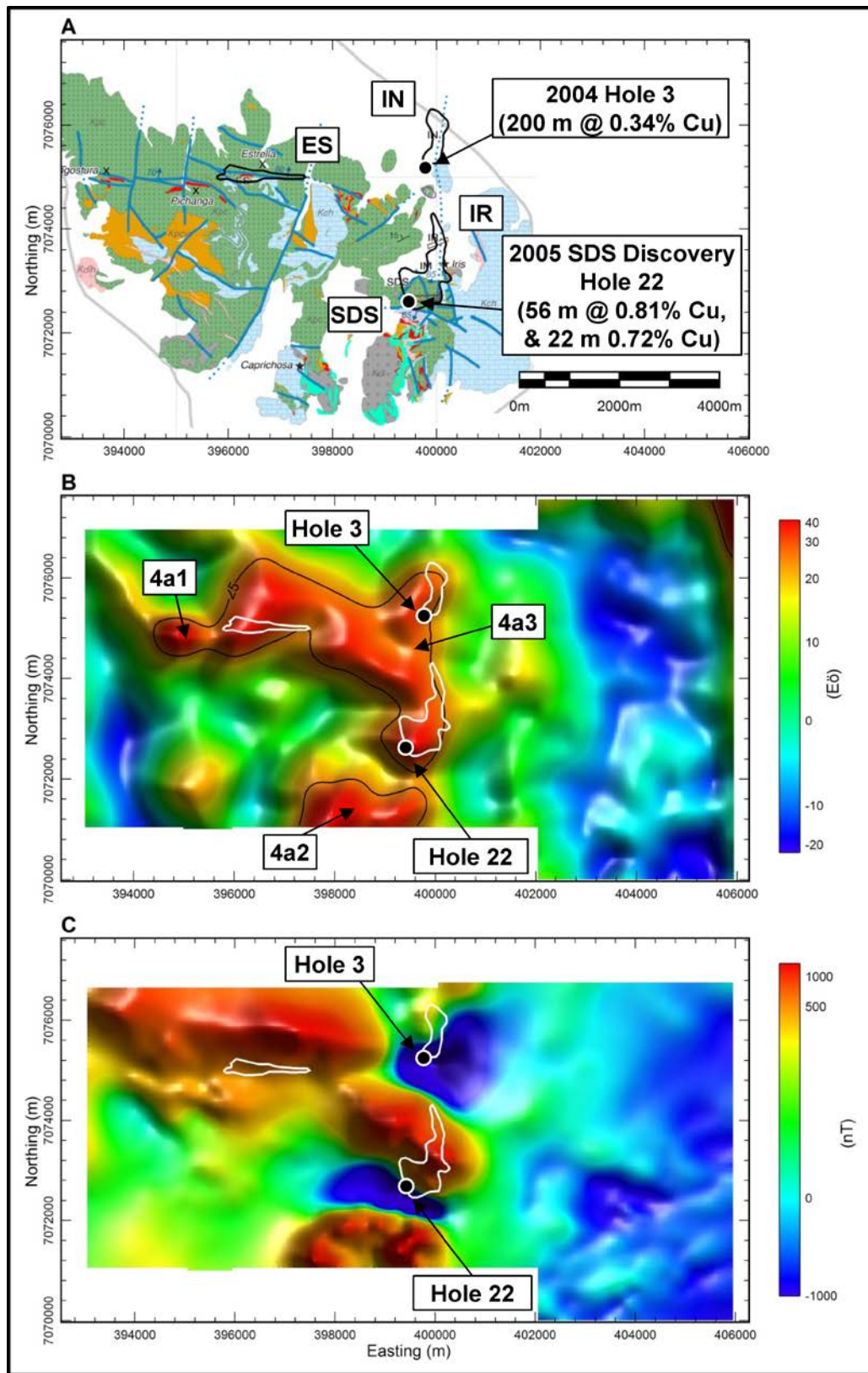
Figure 6: Property Geology after Daroch (2011) showing deposit outlines (A) and RC drill-holes, Falcon AGG gDD (2.90 g/cc terrain correction) with a contour at 25 Eö (B), and Falcon TMI-RTP (C).
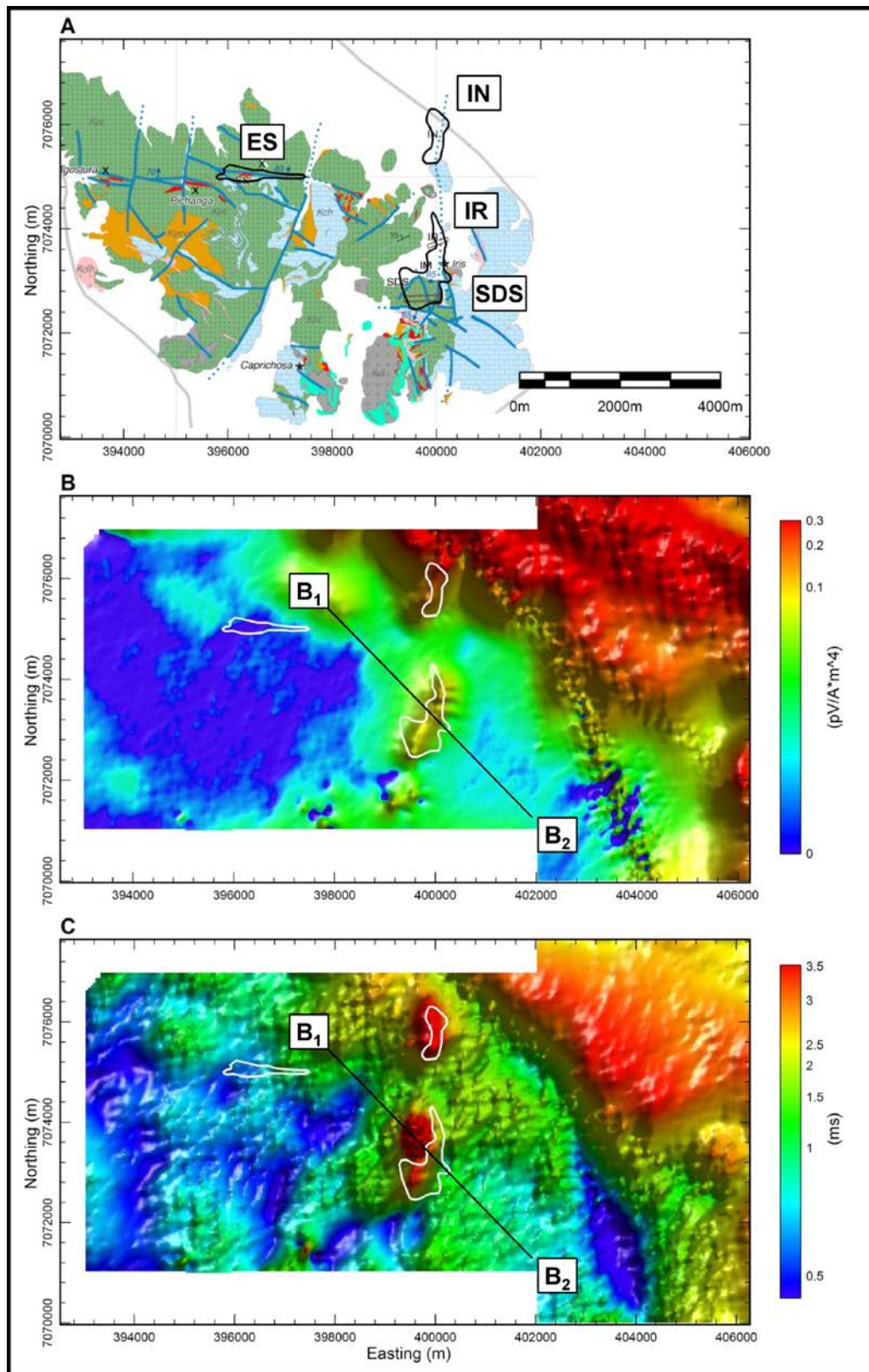
Figure 7: Property Geology after Daroch (2011) showing deposit outlines (A), VTEM dB/dt Z-coil amplitude at 3.521 ms (B), VTEM dB/dt Z-coil Adaptive Tau (noise limit 0.002 pV/(A*m^4)) (C). Black line represents the extent of section B_1 to B_2.
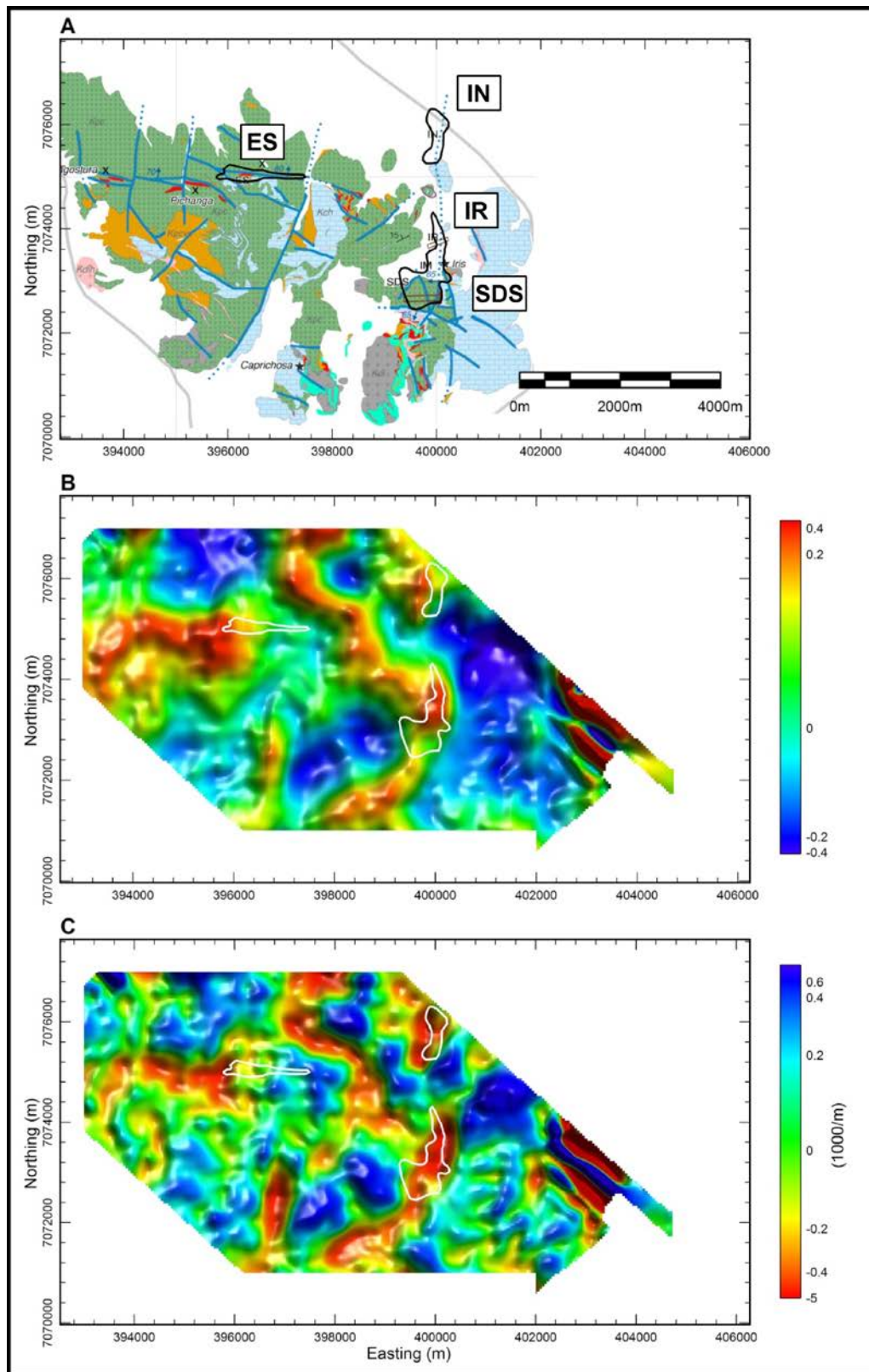
Figure 8: Property Geology after Daroch (2011) showing deposit outlines (A), ZTEM In-phase 75 Hz TPR (B), ZTEM In-phase 75 Hz DT (C).

A section through the SDS-IR ore bodies (between points B_1 and B_2) is presented in Figure 10. The stacked VTEM profiles (A) show a double-peak response with an apparent dip towards the northwest. The apparent dip from the profiles is consistent with the dip obtained from conductive plate modelling and the dip of the high-conductivity zone shown in the VTEM conductivity depth section or CDS (B). There are significant artifacts in the CDS due to limitations of the 1D inversion. However, dip estimates from these images have been found reliable where the source dip is less than 30°.

The IN deposit, though resolved well in the south, is lost in a higher amplitude background response to the north. In both the response amplitude and AdTau, there is a strong contrast between higher elevation area with exposed bedrock (relatively low amplitude/time-constant) and lower elevation areas with cover (generally relatively high amplitude/time-constant). The 1D conductivity inversion indicates a typical conductivity of less than 10 mS/m in the host volcanics, and less than 150 mS/m in the SDS and IR deposits. There is no significant conductivity contrast between the orebody and the host in the areas under cover where 150 mS/m and greater conductivity is ubiquitous. The highest amplitude late-time responses in the survey area do not correlate with the deposits but rather areas of alluvial and fluvial material in the valley. The VTEM data are useful to resolve the deposits where a high-copper sulphide tenor is present but only in the absence of the relatively conductive cover.

2013 ZTEM Survey

The heliborne ZTEM survey was flown immediately after the first phase of the VTEM survey using an identical flight plan excepting two lines in the northeast which were removed based on review of the VTEM power line monitor data. The mean AFMAG sensor terrain clearance in the area shown was 103 m. The acquisition and processing of the AFMAG and total field magnetic data were completed by Geotech (Venter et al., 2013) with additional processing, inversions, and modelling completed by Condor. Among other products, Condor generated 3D conductivity inversions using the UBC-GIF MTZTEM code (Cunion, 2014).

The Geotech Total Phase Rotated (TPR) and Total Divergence (DT) grids (Lo et al., 2009) for the 75 Hz in-phase Tipper responses are shown in Figure 8. The SDS-IR and IN ore bodies are correlated with high and low responses in the TPR and DT, respectively, indicating relative low-resistivity regions. The ES orebody is correlated with a resistive zone while the area of the minor mantos to the west is correlated with a lower resistivity zone.

Contacts and faults not captured in the gridded VTEM amplitude and AdTau data appear to correlate with features in the TPR and DT grids. The Kch sedimentary units correlate with relatively high-resistivity zones and indicate a likely extension of the Kch. Kpcvs also appear to be relatively resistive but perhaps less so than the Kch. The intrusive diorites are correlated with a low-resistivity response and the response between SDS-IR and IN is roughly continuous.

The 3D conductivity inversion of the ZTEM results compares favourably with 1D inversions of the VTEM. In Figure 9, sections are presented at a common 300 m below surface though conductivity models derived from the VTEM (B) and ZTEM (C) data. Both of the conductivity sections are broadly similar (the linear high conductivity zone along the northeast and the arcuate high in the east of the ZTEM sections are likely power line noise). The SDS-IR and IN ore bodies are resolved as relatively conductive zones though they appear better isolated in the VTEM inversion. In Figure 10, the ZTEM in-phase and quadrature Tipper T_{ZX} profiles are shown for all useful frequencies (C) above a vertical section through the ZTEM 3D conductivity model (D). The profiles show a typical conductive response over SDS with the in-phase cross-over located at approximately the same location as the VTEM pick and as the peak TMI-RTP response (E). While the conductive zones in both the VTEM and ZTEM derived CDS are similar and a common direction of dip is indicated, the conductive zone in the ZTEM 3D conductivity inversion appears to be more reliable with a peak conductivity centred at the deposit location and plausible conductor morphology.

Comparison of Airborne and Ground Geophysical Data over SDS-IR and IN

Ground DC IP data were acquired along an irregular set of lines in 2004 using a pole-dipole electrode configuration, an a-spacing of 100 m and n-values from 1 to 6. An Iris IP6 receiver was paired with a 3 kW transmitter, and a 5 kW generator (Pystynen, 2004). Several lines with what appear to be reliable resistivity inversions were recovered from the data archive and images of the 2D sections were located in 3D. A line through the south of the SDS orebody shows a low-resistivity zone consistent with a low-resistivity zone recovered in the ZTEM inversion and the location of the ore shell. Chargeability highs are ubiquitous across the section both inside and outside the deposit area.

The ground moving-in-loop TEM survey (Pystynen, 2007) consists of an irregular distribution of survey lines designed to satisfy both engineering and exploration requirements over a large number of targets. The survey was carried out at a 25 Hz base frequency, 100 m station spacing, using a Geonics EM 37 transmitter with 200 m square transmitter loops paired with a Geonics Protem receiver and 3D-3 receiver. The receiver recorded 20 time-windows from 80 μs to 70 ms (which provides common overlap with the VTEM system up to approximately 10 ms). Despite the irregular distribution of the lines, there is some common coverage with the VTEM over the SDS and IN ore bodies. The airborne data provided considerably better resolution along the common profile due to higher spatial and temporal sample rates. Otherwise, the results and interpretations for the ground TEM and the VTEM are nearly identical. In Figure 11, sections are shown at a common 300 m depth below surface though 1D conductivity inversions of the TEM (A), and VTEM data (C). The SDS-IR ore bodies are clearly present as a high conductivity area in the TEM section though the resolution is limited by the relatively sparse dataset.
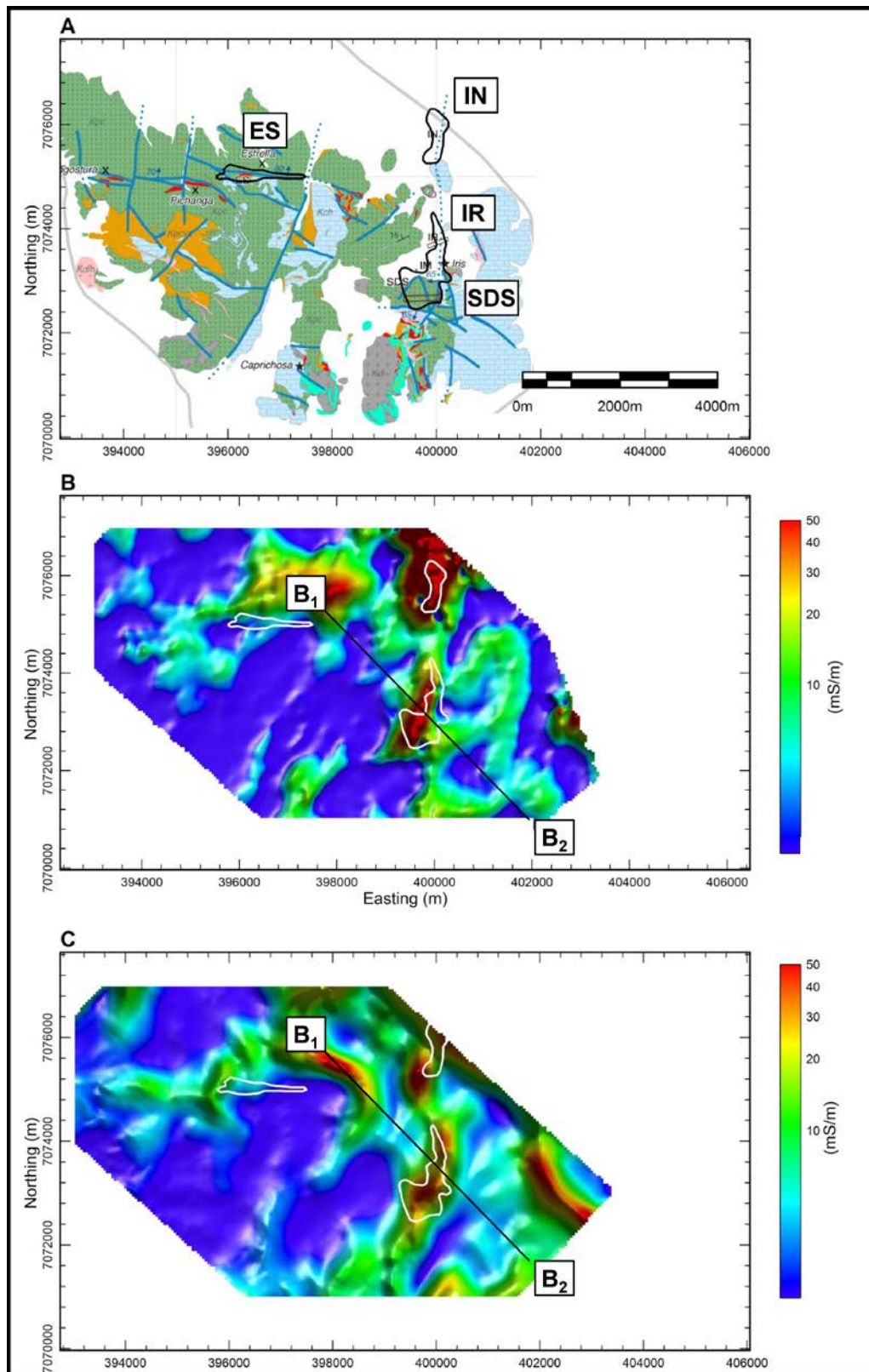
Figure 9: Property Geology after Daroch (2011) showing deposit outlines (A), 300 m depth below surface section through 1D inversion of 25 Hz VTEM (B), 3D inversion of 25 Hz – 600 Hz ZTEM (C). Black line represents the extent of section B_1 to B_2.
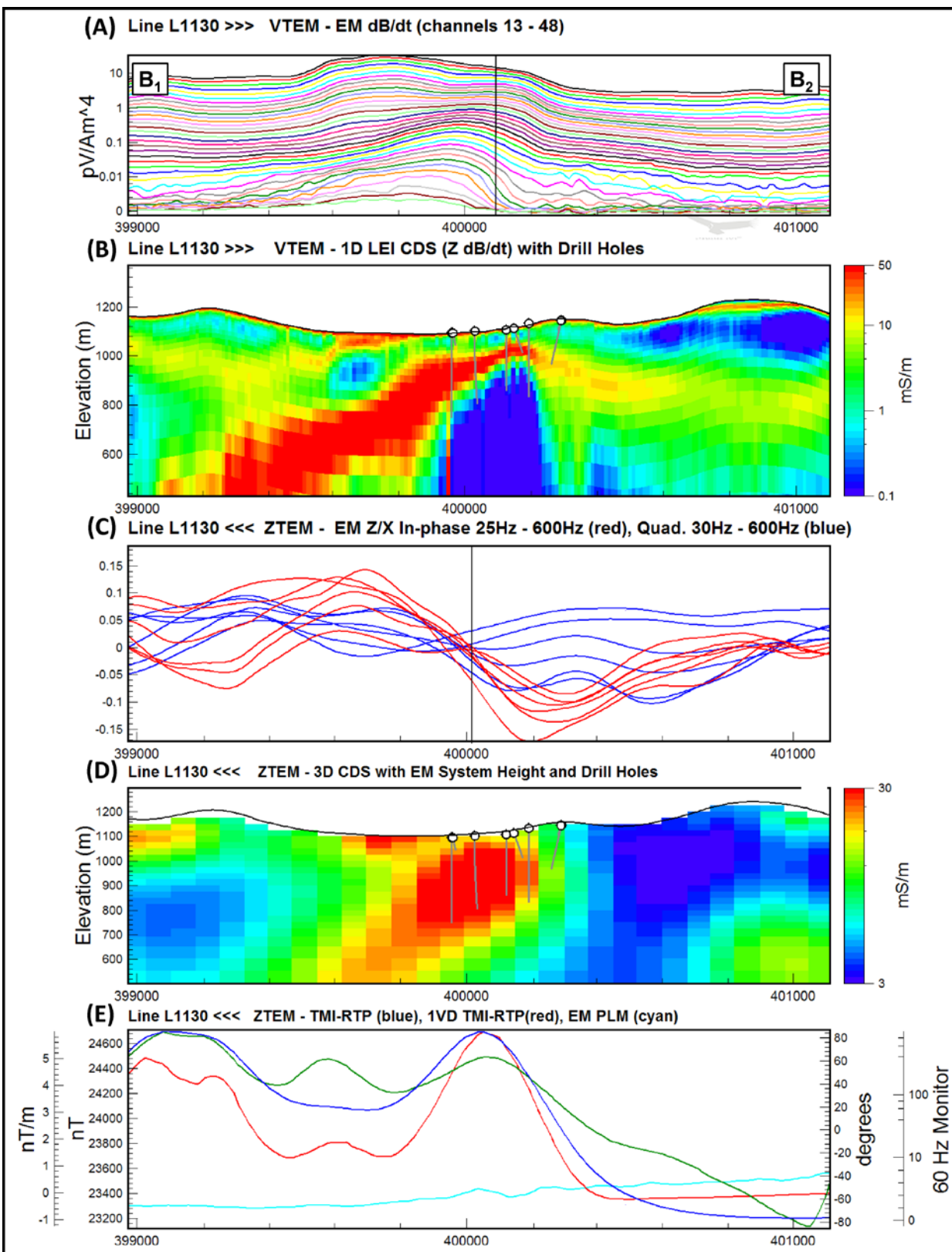
Figure 10: Stacked sections showing VTEM and ZTEM EM and magnetic results on L1130 over the SDS deposit. Centre of conductive source is indicated by a vertical black line. Section width corresponds to the black line between B_1 and B_2 in previous figures.
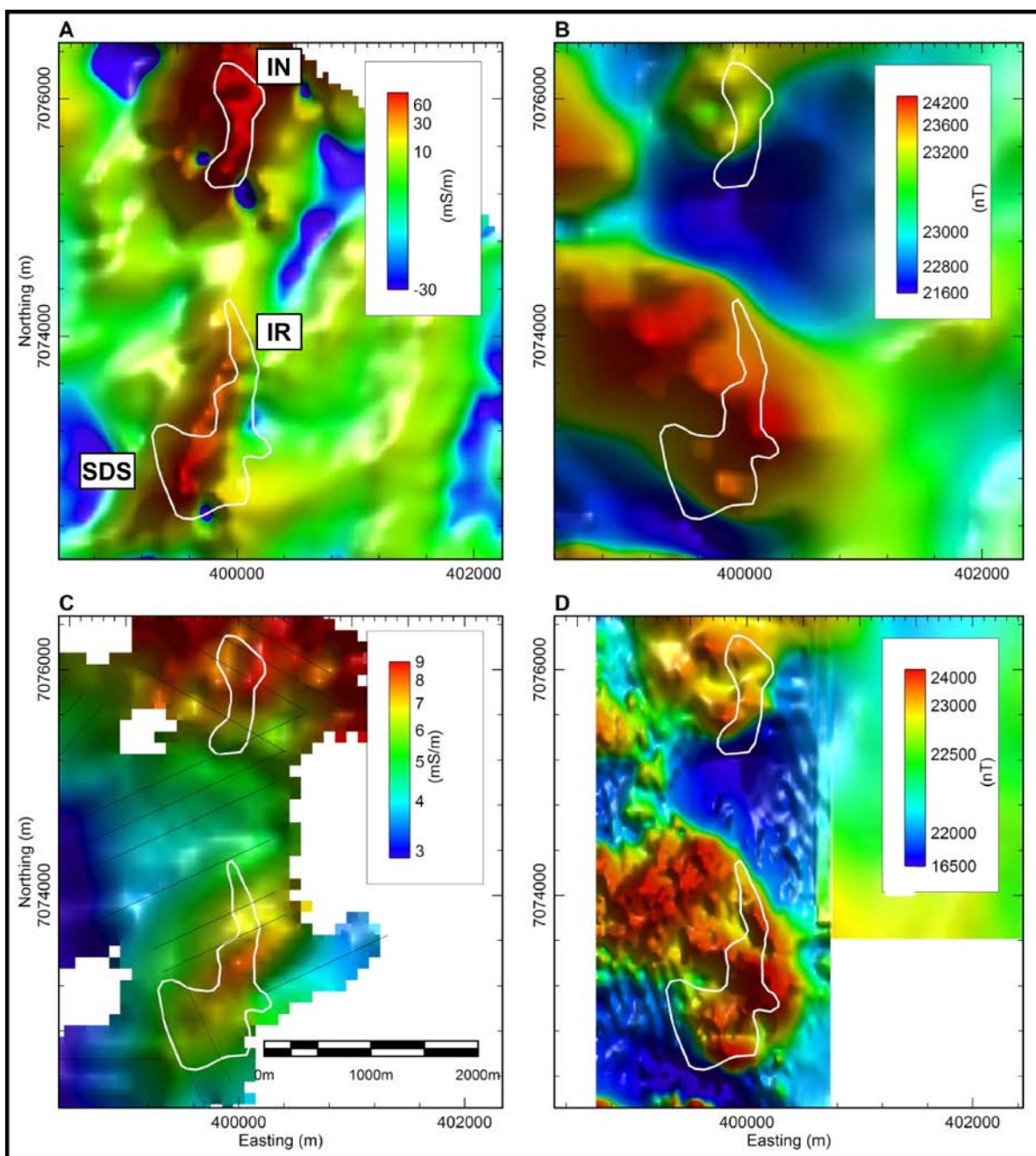
Figure 11: Section at 300 m below surface through 1D inversion of VTEM (A), TMI-RTP merged from VTEM and ZTEM surveys (B), Section at 300 m below surface through 1D inversion of surface 2007 TEM showing survey line locations (C), TMI-RTP merged from ground magnetic survey blocks.

Also in Figure 11, the magnetic data are compared between the TMI-RTP grid generated from the best data acquired during the airborne surveys (B) and from the 2010 ground magnetic survey (D) (Pystynen, 2011). The ground data were acquired at 10 m stations along 100 m space lines in the west and 500 m spaced lines in the east (partially hidden by the colour bar). The ground TMI-RTP is very similar to the airborne grid despite the more than 100 m difference in sensor terrain clearance. The tighter line spacing and ground level sensor location has resulted in

much better resolution overall and appears to more accurately define the south and east contacts at SDS-IR.

CONCLUSIONS

Based on the 2014 review by Condor (Cunion, 2014), all airborne and ground methods except radiometrics were found to map the SDS-IR and IN ore bodies and are of value for the purpose of exploration on the property scale. None of the methods were successful in directly resolving the ES. There

were varying degrees of effectiveness and efficiency to the different methods.

The Falcon gravity (gDD) data were effective in isolating the high density zone designated 4a on a regional scale and then in isolating the individual target areas 4a1, 4a2, and 4a3 all of which correlate to mapped lithologies expected to be relatively dense. While the AGG data were not effective in differentiating mineralized lithologies from barren zones, they were useful for defining faults which contribute to control on the distribution of the copper mineralization.

The total field magnetic data from the various airborne and ground surveys were found to have a good positive correlation. The lack of consistent relationship between the TMI-RTP response in the areas of SDS-IR and IN is plausibly due to remanence as measured in the iron-oxide rich manto at SDS. On the property scale, the magnetic method was more effective for discrimination of faults and contacts than the airborne gravity. The results of the ground magnetic survey indicate that better mapping of structures and contacts is accomplished using higher resolution data than available from the existing airborne datasets.

Airborne VTEM and ground TEM were both very effective in directly detecting the sulphide mineralization at SDS-IR and IN and ineffective at detecting the low-sulphide mineralization at ES. The TEM method can be used to discriminate between magnetic and gravity high responses associated with barren iron-oxide mineralization and deposits with high-sulphide tenor. However, the effectiveness of TEM (at least up to approximately 10 ms off-time) was found to be limited in areas of conductive cover. The effectiveness of TEM as a regional exploration tool depends greatly on the presence of sulphides in the target model and the absence of a conductive host or surficial cover.

The VTEM was of some value in designing the following ZTEM survey. With the assistance of the power line monitor data from the VTEM survey costs were modestly reduced by removing ZTEM survey lines which would have suffered overwhelming noise issues.

While the VTEM products showed the ore bodies as well isolated conductors there was little differentiation of the relatively resistive host rocks, or location of contacts, and faults. The ZTEM products included significantly more of these features while also satisfying the primary criteria of resolving the SDS-IR and IN ore bodies (though the conductive sources were not as well isolated as in the TEM products). The 3D conductivity inversion from the AFMAG data resulted in a plausible morphology for the SDS orebody.

The combination of geophysical data acquired by Far West, BHP Billiton, and Capstone has great utility for identifying all of the deposits at SD. However, due to the incremental acquisition over 12 years, both pre- and post-discovery, the actual exploration value of the geophysical data was diminished. The discoveries at SD were predicated on the concept of exploring the CIB for IOGC deposits using the Falcon system. In this much at least, the Falcon system played a critical role in the exploration effort. The systematic follow-up of the airborne geophysical anomalies with ground mapping and persistent drilling was critical to the success of the exploration program.

Despite the location of early RC drill holes based (as least in part) on the location of chargeability anomalies, the ground geophysics does not appear to have played a significant role in the exploration effort. Rather, ground mapping of alteration, mineralization and faults along with use of the airborne geophysics appears to have been the driver for the discovery at SDS.

The subsequent clear resolution of the SDS-IR and IN deposits using airborne TEM and AFMAG systems suggests that both the discovery and drilling-off of the deposit may have been accelerated if similar EM coverage were available earlier in the exploration process.

REFERENCES

Allen, G.J., 2005, Report on the Exploration Activities in the 4a (Santo Domingo) Area of the Candelaria Project, Region III, Chile: Confidential report prepared for Far West Mining Ltd. and BHP Billiton, April 20, 2005.

Austin, J., D. Clark, P. Schmidt, D. Hillan, and C. Floss, 2013, Magnetic anomalies to mines: Practical insights into the myths, methods and mysteries in relating mineralisation to magnetisation: ASEG Extended Abstracts 2013, 6 p.

Austin, J., D. Hillan, S. Geuna, and D. Clark, 2012, Magnetic modelling of the Candelaria IOCG deposit, Chile: The influence of Remnant Magnetism and Self-demagnetisation: Poster presented at SEG 2012. Available from CSIRO.

Beggerow, L., 2013, The Discovery and Geology of the Santo Domingo IOCG Deposit in Chile: Presentated at PDAC 2013.

Benavides, J, T.K. Kyser, and A.H. Clark, 2007, The Mantoverde iron oxide-copper-gold district, III Región, Chile: the role of regionally derived, nonmagmatic fluids in chalcopyrite mineralization: Economic Geology, 102(3), 415-440.

Cunion, E., 2014, Assessment of the Santo Domingo Airborne and Ground Geophysical Surveys, Chile for Minera Santo Domingo, June, 2014: Confidential report to Capstone Mining Corporation by Condor Consulting, Lakewood, Colorado, USA.

Daroch, G., 2011, Hydrothermal Alteration and Mineralization of the Iron Oxide (-Cu-Au) Santo Domingo Sur Deposit, Atacama Region, Northern Chile: MSc thesis, University of Arizona.

Daroch, G., and M. Barton, 2011, Hydrothermal Alteration and Mineralization in Santo Domingo Sur Iron Oxide (-Cu-Au) (IOCG) Deposit, Atacama Region, Chile: Proc. 11th Biennial SGA Meeting, 488-490.

Far West Mining Ltd., 2005, Management's Discussion and Analysis for the financial year ended December 31, 2005.

Fiset, N, T. Eadie, and G. Plastow, 2014a, Report on a Helicopter-Borne Versatile Time Domain Electromagnetic (VTEM Plus) and Aeromagnetic Geophysical Survey. Santo Domingo Test Block, Diego de Almargo, Chile: Report for Capstone Mining Corp. by Aeroquest Airborne. Project AQ130222-1, January, 2014.

Fiset, N, O.M.T. Eadie, and G. Plastow, 2014b, Report on a Helicopter-Borne Versatile Time Domain Electromagnetic (VTEM Plus) and Aeromagnetic Geophysical Survey. Santo Domingo Test Block and Extension Block, Diego de Almargo, Chile: Report for Capstone Mining Corp. by Aeroquest Airborne. Project AQ130222-4, May, 2014.

Grocott, J., and G. Taylor, 2002, Magmatic arc fault systems, deformation partitioning and emplacement of granitic complexes in the Coastal Cordillera, north Chilean Andes (25°30' to 27°00' S): Journal of the Geological Society of London, 159, 425–442.

Hart, J., and H. Freeman, 2003, Geophysics of the prominent hill prospect, South Australia: ASEG Extended Abstracts 2003, 93-100.

Hensley, C., 2002, Canregional Blocks 1, 2, 3, 4. Falcon Interpretation Report, Candelaria Belt, Coastal Cordillera, Chile: BHP Billiton Confidential Report number 10533.

Hindson, R., 2005a, Far West Mining Ltd. provides update on exploration projects in Chile, Argentina, and Australia: June 1, 2005 News release for Far West Mining Ltd. Available on SEDAR.

Hindson, R., 2005b, Drilling in the 4a3 Target Area of Far West Minings Ltd's Candelaria Project Intersects Significant IOCG Mineralization: July 21, 2005 News release for Far West Mining Ltd. Available on SEDAR.

Lara, L., and E. Godoy, 1998, Hoja Quebrada Salitrosa, III Región de Atacama: Santiago, Chile, Servicio Nacional de Geología y Minería: Mapas Geológicos 4, scale 1:100.000.

Lo, R., J. Legault, P. Kuzmin, and M. Combrick, 2009, ZTEM (airborne AFMAG) tests over unconformity uranium deposits: ASEG Extended Abstracts 2009.

Maksaev, V., B. Townley, C. Palacios, and F. Camus, 2007, Metallic ore deposits, in T. Moreno, and W. Gibbons eds., (The Geology of Chile, 179 – 199.

Marschik R, R.A. Leveille and W. Martin, 2000, La Candelaria and the Punta del Cobre district, Chile. Early Cretaceous iron oxide Cu-Au(-Zn-Ag) mineralization, in. T.M. Porter ed., Hydrothermal iron oxide copper-gold and related deposits: A global perspective, Australian Mineral Foundation, Adelaide, 163–175.

Matthews, J, and Jenkins, R, 1997. Geophysical Exploration and Discovery of the Candelaria Copper-Gold Deposit in Chile, in A. Gubins, ed., Proceedings of Exploration 97, 983–992.

Maycock, J, D. Frost, V. Khera, C. Guzman, R. Betinol, H. Gopfert, A. Klimek, D. Rennie, and T. Kerr, 2014, Santo Domingo Project, Region III, Chile, NI 43-101 Technical Report on Feasibility Study: for Capstone Mining Corporation. Project Number M40206. Available on SEDAR.

McCleary, A., 2003, Project Report Aeromagnetic, radiometric, and airborne gravity gradiometer survey: Candelaria Regional Blocks 1 to 8, Copiapo, Chile, 2002. Logistics and Processing report for BHP Billiton by Sander Geophysics Ltd. SGL Project Numbers 215, 253-256, 270-272: Unpublished confidential report.

Moul, F, P. Paré, and E. Cunion, 2016, Comparison of VTEM and ZTEM Results over the Santo Domingo IOCG Deposit, Region III, Chil: Presentation at Geotech Vancouver Geophysics Symposium.

Parada, M.A., L. Lopez-Escobar, V. Oliveros, F. Fuentes, D. Morata, M. Calderon, L. Aguirre, G. Feraud, F. Espinoza, H. Moreno, O. Figueroa, J.M. Bravo, R. Troncosco Vasquez and C.R. Stern, 2007, Andean magmatism, in T. Moreno, and W. Gibbons, W. eds., The Geology of Chile, 115 – 146.

Paré, P, F. Moul, and E. Cunion, 2016, An Assessment of Airborne and Ground Geophysics over the Santo Domingo IOCG Deposit, Region III, Chile: Presentation at Geotech Geophysics Symposium.

Pystynen, A., 2004, Geophysical Report on the Induced Polarization and Resistivity Surveys conducted at the Candelaria Copper Belt Projects, Regions II and III, Chile: Confidential report to Far West Mining Ltd. by Quantec Geofisica Ltda. Project number C-484, March, 2005.

Pystynen, A., 2007, Geophysical Logistics Report on the Transient Electromagnetic (TEM) Surveys conducted at the Santo Domingo Project Region III, Chile: Confidential report for Minera Lejano Oeste S.A. by Quantec Geoscience Chile. Project number C-558. November, 2007.

Pystynen, A., 2011, Geophysical Logistics Report on the Ground Magnetic Surveys conducted at the IOCG Phase 2 Projects, Region III, Chile: Confidential report for Far West Exploration S.A. by Quantec Geoscience Chile Ltda., Project number QGC-650, January, 2011.

Ryan, P, A. Lawrence, R. Jenkins, J. Matthews, J. Zamora, M. Enrique, and I. Diaz, 1995, The Candelaria Copper-gold Deposit, Chile, in F. Pierce, and J. Bolm, J eds., Porphyry Copper Deposits of the American Cordillera, Arizona Geological Society Digest, 20, 625-645.

Sillitoe, R., 2003, Iron oxide-copper-gold deposits: an Andean review: Mineralium Deposita, 38, 787-812.

Vella, L, and D. Emerson, 2012, Electrical Properties of Magnetite- and Hematite-Rich Rocks and Ores: ASEG Extended Abstracts 2012, 4 p.

Vila, T, N. Lindsay, and R. Zamora, 1996, Geology of the Manto Verde copper deposit, northern Chile: a specularite-rich, hydrothermaltectonic breccia related to the Atacama Fault Zone, in F. Camus, R. Sillitoe, and R. Petersen, R. eds., Andean Copper Deposits: New Discoveries, Mineralization Styles and Metallogeny: Society of Economic Geologists, Special Publication 5, 157–170.

Vivallo, W and F. Henriquez, 1998, Génesis común de los depósitos estratoligados y vetiformes de cobre del Jurásico Medio a Superior en la Cordillera de la Costa, Región de Antofagasta, Chile: Revista Geológica de Chile, 25, 199–228.

Venter, N, G. Plastow, A. Latrous, and J. Legault, 2013, Report on a Helicopter-Borne Z-axis Tipper Electromagnetic (ZTEM) and Aeromagnetic Geophysical Survey. Santo Domingo Block, Diego de Almagro, Chile: Confidential report for Capstone Mining Corp. by Aeroquest Airborne, Project AQ130442, December, 2013.

Zamora, R., and B. Castillo, 2001, Mineralización de Fe-Cu-Au en el distrito Mantoverde, Cordillera de la Costa, III Región de Atacama, Chile: Congreso Internacional de Prospectores y Exploradores, Lima, Conferencias, 2nd, Instituto de Ingenieros de Minas del Perú, Lima.

Zonge International Inc., 2011, Petrophysics Laboratory Results Summary, Remnant Magnetization Analysis: Spreadsheet without accompanying documentation.